V.A.1 Fuel Cell Systems Analysis

Rajesh K. Ahluwalia (Primary Contact), Xiaohua Wang, Kazuya Tajiri, Romesh Kumar
Argonne National Laboratory
9700 South Cass Avenue
Argonne, IL 60439
Phone: (630) 252-5979; Fax: (630) 252-5287
E-mail: walia@anl.gov

DOE Technology Development Manager: Nancy Garland
Phone: (202) 586-5673; Fax: (202) 586-9811
E-mail: Nancy.Garland@ee.doe.gov

Project Start Date: October 1, 2003
Project End Date: Project continuation and direction determined annually by DOE

Objectives

- Develop a validated model for automotive fuel cell systems, and use it to assess the status of the technology.
- Conduct studies to improve performance and packaging, to reduce cost, and to identify key research and development issues.
- Compare and assess alternative configurations and systems for transportation and stationary applications.
- Support DOE/FreedomCAR automotive fuel cell development efforts.

Technical Barriers

This project addresses the following technical barriers from the Fuel Cells section of the Hydrogen, Fuel Cells, and Infrastructure Technologies Program Multi-Year Research, Development and Demonstration Plan:

(B) Cost
(C) Performance
(E) System Thermal and Water Management
(F) Air Management
(G) Startup and Shutdown Time and Energy/Transient Operation

Technical Targets

This project is conducting system level analyses to address the following DOE 2010 and 2015 technical targets for automotive fuel cell power systems operating on direct hydrogen:

- Energy efficiency: 50%-60% (55%-65% for stack) at 100%-25% of rated power
- Power density: 650 W/L for system, 2,000 W/L for stack
- Specific power: 650 W/kg for system, 2,000 W/kg for stack
- Transient response: 1 s from 10% to 90% of rated power
- Start-up time: 30 s from –20°C and 5 s from +20°C ambient temperature
- Precious metal content: 0.3 g/kW (2010), 0.2 g/kW (2015)

Accomplishments

- Worked with 3M to analyze the performance of stacks with nanostructured thin film catalysts (NSTFCs) with reduced Pt loading and at elevated temperatures.
- Built and validated the performance maps for the different components of the Honeywell's integrated compressor-expander-motor module (CEMM) and analyzed the performance of the CEMM.
- Analyzed the performance of advanced automotive radiators with high-density louver and plain microchannel fins. Identified a compact radiator design with the lowest parasitic air pumping power.
- Assisted Honeywell in determining the performance of full-scale enthalpy wheel and membrane humidifiers (MHs).
- Determined the time and energy for startup and shutdown of polymer electrolyte fuel cell stacks at different stack and ambient temperatures.
- Conducting drive cycle simulations to determine the fuel economy of hybrid fuel cell vehicles.

Introduction

While different developers are addressing improvements in individual components and subsystems in automotive fuel cell propulsion systems (i.e., cells, stacks, balance-of-plant components), we are using modeling and analysis to address issues of thermal and water management, design-point and part-load operation, and component-, system-, and vehicle-level efficiencies and fuel economies. Such analyses are essential for effective system integration.

Approach

Two sets of models are being developed. The GCtool software is a stand-alone code with capabilities for design, off-design, steady state, transient, and constrained optimization analyses of fuel cell systems (FCSs). A companion code, GCtool-ENG, has an alternative set of models with a built-in procedure for translation to the MATLAB/SIMULINK platform commonly used in vehicle simulation codes such as PSAT.

Results

In Fiscal Year 2009, we changed our reference FCS configuration (see Figure 1) to provide for cooling of the motor and airfoil bearings (AFBs) in the CEMM, and replaced the enthalpy wheel humidifier with a membrane humidifier for the cathode inlet air [1]. The revised configuration also includes an air precooler upstream of the MH for improved MH durability and performance.

Air Management

We analyzed data received from Honeywell and constructed performance maps for the mixed axial flow compressor, variable area nozzle turbine (VNT), 3-phase brushless direct current motor, and liquid-cooled motor controller [2]. We also developed correlations for the motor and AFB cooling loads and pressure drops for the motor/AFB cooling air and the CEMM air filter. The maps were used to model the performance of a matched compressor, expander, and motor on a common shaft for the 80-kW reference FCS: 2.5 bar at rated power, 90°C stack temperature, 91 g/s dry air flow rate, and 3 psi pressure drop between the compressor exit and turbine inlet. We determined the VNT nozzle area and shaft rpm to control the stack inlet relative humidity (RH) with a membrane humidifier. Figure 2 presents the modeled operating map of the CEMM and the component efficiencies. The calculated peak efficiencies are 70.3% for the compressor, 73.2% for the expander, 86% for the motor and 87.3% for the motor controller, which may be compared with the efficiency targets of

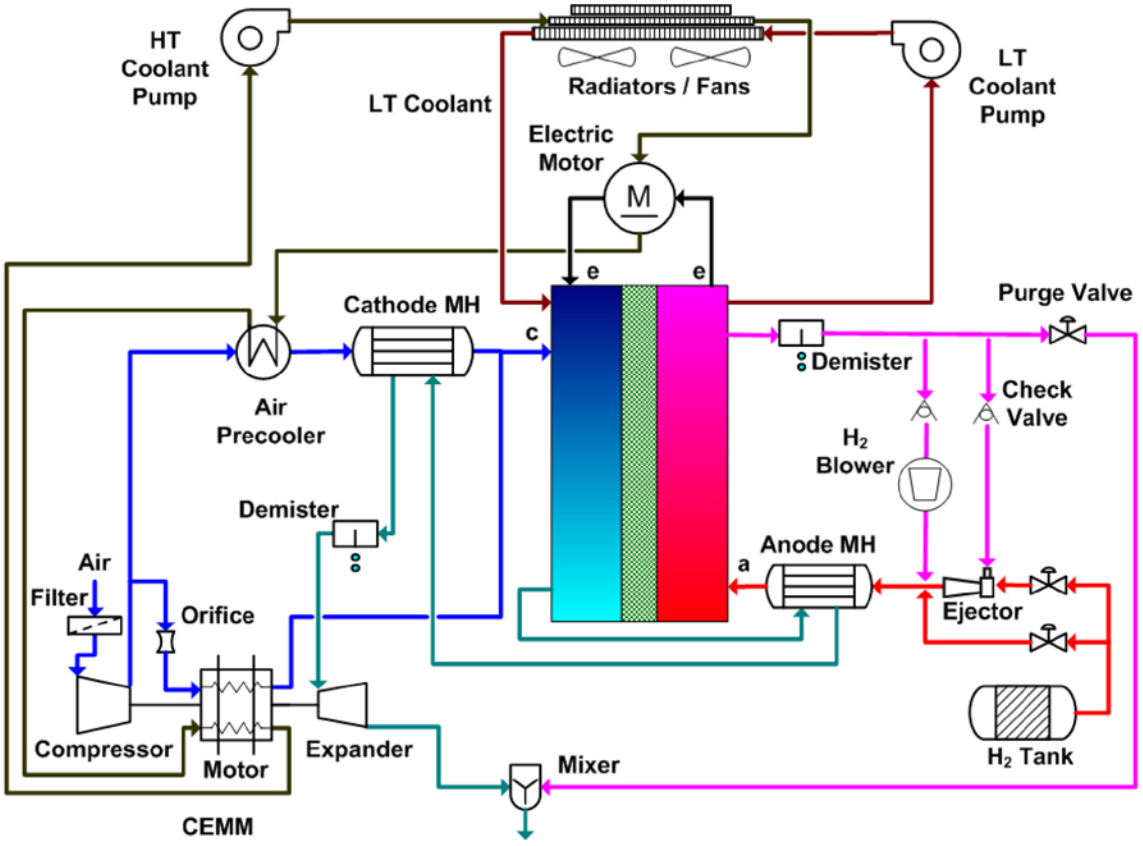

HT - high temperature; LT - low temperature

FIGURE 1. Reference Pressurized FCS with Motor Cooling and Membrane Humidifier

80% each for the compressor and the expander, and 92% each for the motor and the motor controller. We calculate that for the FCS at rated power, the CEMM will consume about ~9 kW at 300 K ambient temperature, significantly higher than the target power consumption of 4.4 kW.

Fuel Cell Stack Performance

We received 3M single-cell data for the electrochemical surface area, specific activity, short and crossover currents and high frequency resistance over a wide range of temperatures (80–120°C) and RHs (20–100%) [3]. The data, obtained with 0.1(a)/0.15(c) mg/cm^2 Pt loading and 35-μm-thick membrane (850 equivalent weight), provided a basis for formulating a kinetic model for the oxygen reduction reaction (ORR) on the nanostructured thin film ternary PtCoMn catalyst that is valid at elevated temperatures and under dry conditions. The ORR kinetics model was used in a trade-off study to determine the stack Pt content (g/kW) as a function of the operating pressure, temperature and inlet RH for specified system efficiency (50%), oxygen utilization (50%) and per-pass hydrogen utilization (70%). The results from the study (Figure 3) showed that for a given stack inlet pressure, the Pt content is at a minimum corresponding to an optimum level of RH that is a function of the stack operating temperature (e.g., 40% RH at 90°C and 2.5 bar). The higher the stack temperature, the higher is the optimum RH. Moreover, for a given stack inlet pressure there is an optimum combination of stack temperature and RH that leads to a minimum Pt content (100°C and 50% RH at 2.5 bar). In practice, however, the maximum stack operating temperature will likely be limited by the membrane and catalyst durability concerns.

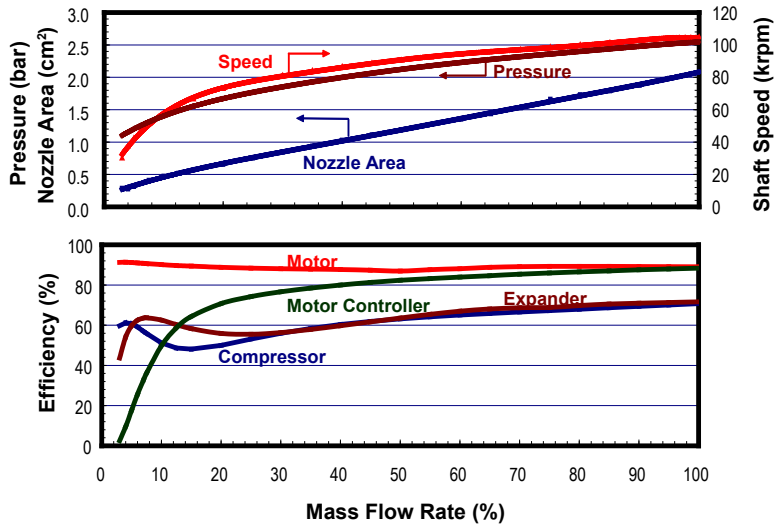

FIGURE 2. Performance of Integrated CEMM with VNT and Motor Cooling

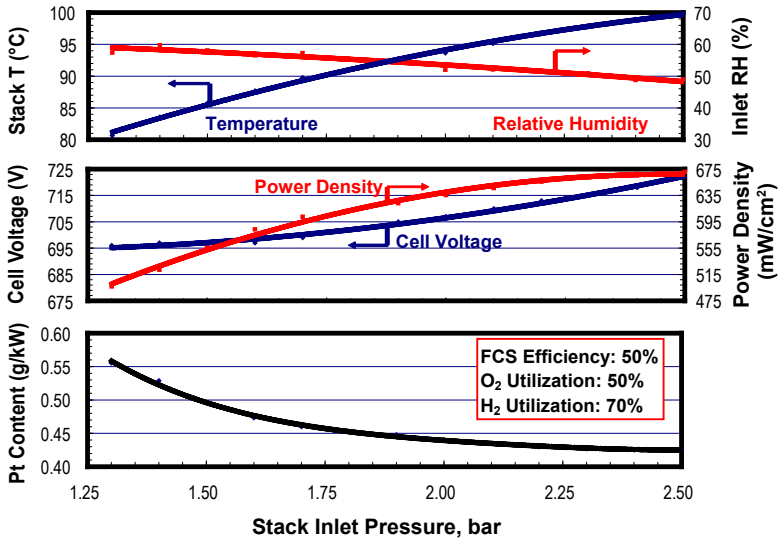

FIGURE 3. Effect of NSTFC Stack Operating Pressure on Temperature and RH (a), Pt Content (b) and Power Density (c)

The study was expanded by varying the stack pressure over the range 1.25 to 2.5 bar. The optimum combinations of stack temperature and inlet RH were determined as a function of the stack inlet pressure. We found that the optimum stack temperature increases, and the inlet RH decreases, as the stack inlet pressure is raised. For the conditions of this study, the optimum combination of temperature and inlet RH is 94°C and 52% at 2 bar and 82°C and 58% at 1.3 bar. We calculated that the air management system consumes 9 kW to deliver air at 2.5 bar stack inlet pressure but only 5.2 kW if the stack inlet pressure is reduced to 1.3 bar. As a result, the stack operating at 2.5 bar has to generate ~3.8 kW additional power to compensate for the larger parasitic losses (constant 80 kW net system power) and to operate at ~30 mV higher cell voltage to maintain constant 50% system efficiency. In spite of these drawbacks, the stack power density is 35% higher at 2.5 bar than at 1.3 bar operating pressure and the overall Pt content is ~30% lower. This study leads to the conclusion that from the standpoint of reducing the overall Pt content (i.e., reducing the system cost), it is preferable to operate the NSTFC stack at a moderately high pressure (2.5 bar) than at low or near ambient pressures.

Thermal Management

We received and analyzed the thermal and fluid mechanics data from Honeywell for 9"x9" subscale radiators with 18 and 24 fpi (fins per inch) louver fins (LV) and 40 and 50 fpi plain microchannel (MC) fins [4]. We derived the friction factor (f factor) and heat transfer (j factor) coefficients from the data, formulated correlations for the f and j factors, and incorporated these correlations in our automotive radiator model. We compared the relative performance of the four fin geometries tested and concluded that the LV-24 fins are preferable to the LV-18 fins, and that the MC-40 fins are superior to the MC-50 fins. Our preliminary assessment of the 24-fpi louver and 40-fpi microchannel fins is that for a given frontal area ($A_{ref} = 0.25\ m^2$), heat load (50 kW at 55 mph) and reference grill and under-hood fluid mechanics parameters, the LV-24 fins require lower fan power but the radiator with MC-40 fins can be more compact.

We conducted a study to assess the heat rejection in fuel cell vehicles as a function of the stack and ambient temperatures. We considered that the air-conditioning condenser (8.5 kW heat load) and the low-temperature radiator (9 kW heat load) are stacked in front of the high-temperature radiator that rejects waste heat generated in the fuel cell stack. Figure 4 presents some of the results from the study for LV-24 fins. It shows that for a given frontal area, there is an optimum radiator depth that leads to minimum fan pumping power. The fan pumping power is higher for depths larger than the optimum because of higher pressure drop; it is also higher for depths smaller than the optimum because of the smaller heat transfer area and the correspondingly larger air flow requirement. Figure 4 shows that the fan pumping power can be greatly reduced by increasing the frontal area although this may not be feasible in automotive applications. Ambient temperature is seen to have a significant effect on the ability to reject heat. The fan pumping power can more than double with a mere 5°C increase in ambient temperature from 40°C to 45°C. The stack temperature has a similar effect on heat rejection ability. For the same pumping power (300 W), the frontal area increases by 40% if the stack operates at 80°C rather than at 90°C. Conversely, for the same frontal area ($A/A_{ref} = 1.25$), the fan pumping power more than doubles, if the stack operates at 80°C rather than at 90°C.

Water Management

We initiated a study to assess the prospect of meeting the 2010 target requiring unassisted start from –20°C to produce 50% of rated power within 30 s while using <5 MJ energy for startup (and previous shutdown). We formulated a dynamic model for water uptake and transport in the membrane and ionomer in the catalyst layers and used it to analyze startup from subfreezing temperatures (N111 membrane, dispersed Pt/C catalysts, graphite bipolar plates, 1,770 W/kg stack specific power). We found that the initial membrane water content (λ, moles of water in one equivalent weight of the perfluorosulfonic acid membrane) is an important parameter that determines whether a successful self-start is possible. There is a critical λ ($\lambda_h = 7.5$ for startup from –20°C) above which self-start is not possible because the product water completely engulfs the catalyst layers with ice before the stack can warm up to 0°C. There is

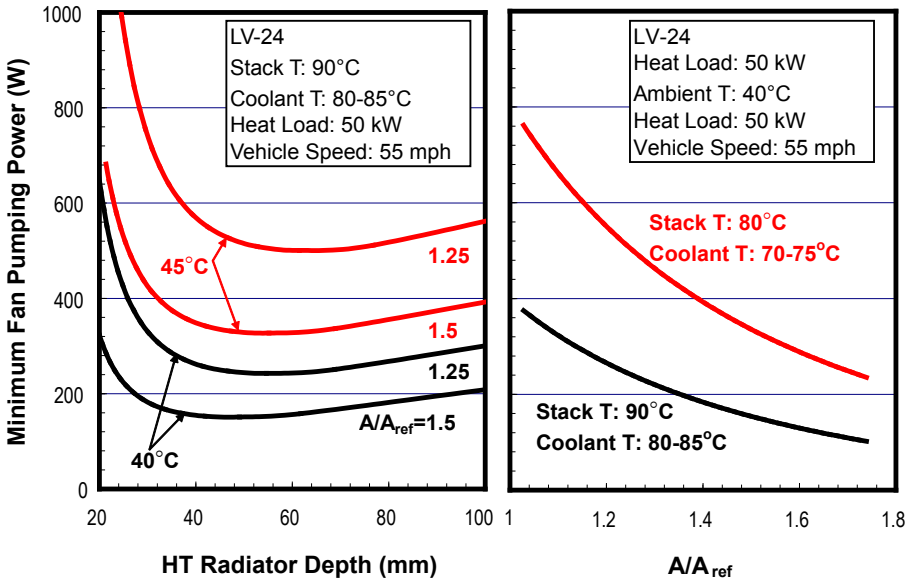

FIGURE 4. Performance of FCS High Temperature Radiator with 24-fpi Louver Fins

a second value of λ ($\lambda_l = 5$) below which the stack can be self-started without forming ice. Between λ_l and λ_h, the stack can be self-started, but with intermediate formation of ice that melts as the stack warms up to 0°C. Both λ_l and λ_h are functions of the initial stack temperature, cell voltage at startup, membrane thickness, catalyst loading, and stack heat capacity. The higher the initial stack temperature and the lower the cell voltage, the higher are λ_l and λ_h. Our simulations show that the startup from a subfreezing temperature is robust for $\lambda < \lambda_l$, since ice does not form as the membrane absorbs the product water during the time that the stack warms up to 0°C. Startup under this condition results in the current density monotonically increasing with time. During startup for $\lambda_l < \lambda < \lambda_h$, the product water is initially absorbed in the membrane until it becomes locally saturated (λ=14 for Nafion®) after which ice begins to form. Thus, startup for $\lambda_l < \lambda < \lambda_h$ results in the current density initially increasing with time and then declining with time. All the product water turns into ice if the initial λ is greater than 14 and the current density monotonically decreases with time.

We have also analyzed the time required and the energy consumed during shutdown in order to prepare the stack for a subsequent successful startup from subfreezing temperatures (i.e., to "dry" the stack to $\lambda_l < \lambda < \lambda_h$). We have run simulations to study the drying of the membrane by purging the cathode with air (no anode purge) as a function of the initial stack temperature and water content of the catalyst and gas diffusion layers (saturation levels). We find that, depending on the initial saturation level, it may not be possible to dry the membrane to the target λ if the stack at the start of the purge cycle is below a certain temperature. This points to a potential problem in that a robust start from subfreezing temperature may be difficult if the prior shutdown occurred after a short drive that resulted in the stack being heated to <30–50°C.

Finally, we have determined the optimum λ for robust and rapid startup and shutdown. Startup and shutdown time and energy may be unacceptable if the λ is much less than the optimum. Conversely, a robust startup from subfreezing temperatures cannot be assured if the λ is much higher than this optimum.

Conclusions and Future Directions

- The Honeywell design of the air management system can reach peak component efficiencies of 70.3% for the compressor, 73.2% for the expander, 86% for the motor, and 87.3% for the motor controller. The VNT allows the module to be adapted to different design pressures.
- Even with the reconfigured design that utilizes the cooling air, the air management system consumes about ~9 kWe to deliver 91 g/s air at 2.5 bar stack inlet pressure for an 80-kWe FCS. Further improvements in aerodynamics are needed to reach the DOE target of no more than 4.4-kW parasitic power.
- We have compared the performance of pressurized and near-ambient pressure FCSs with NSTFCs. We have concluded that in spite of the larger parasitic losses in the air management system and the higher operating cell voltage needed to achieve 50% system efficiency, the Pt content is lower with the pressurized system than with the near ambient pressure system.
- Our analysis of the experimental data for the four types of fins tested on subscale radiators leads us to conclude that the 24-fpi louver fins is the best option from the standpoint of blower pumping power and radiator compactness.
- Initial membrane water content (λ) is an important parameter that determines whether a successful unassisted self-start is possible from subfreezing temperatures. Similarly, the stack temperature prior to shutdown largely determines the time and energy required to dry the membrane to specific values of λ, for which self-start is possible.
- In FY 2010, we will redo the system analysis with reduced Pt loading of 0.1 mg/cm^2(c) and 0.05 mg/cm^2(a). We will consider catalyst and membrane durability in addition to system cost and performance. Also, we will analyze the dynamic performance of the fuel cell system under real-world driving conditions.

FY 2009 Publications/Presentations

1. R.K. Ahluwalia and X. Wang, "Effect of CO and CO_2 Impurities on Performance of Direct Hydrogen Polymer-Electrolyte Fuel Cells," Journal of Power Sources, 180 (2008), 122-131.

2. R.K. Ahluwalia and X. Wang, "Fuel Cell Systems for Transportation: Status and Trends," Journal of Power Sources, 177 (2008), 167-176.

3. H. Adachi, S. Ahmed, S.H.D. Lee, D. Papadias, R.K. Ahluwalia, J.C. Bendert, S.A. Kanner, and Y. Yamazaki, "A Natural-gas Fuel Processor for a Residential Fuel Cell System," Journal of Power Sources, 188 (2009), 244–255.

4. X. Wang, R.K. Ahluwalia and K. Tajiri, "PEMFC Startup from Subfreezing Temperatures: Mechanism, Time and Energy Requirement," PEMFC Freeze Technical Workshop, Nuvera Fuel Cells Inc., Billerica, MA, February 20, 2009.

5. X. Wang and R.K. Ahluwalia, "Dynamics of CO Poisoning of Pt Anodes in PEM Fuel Cells," Fuel Quality Modeling Workshop, National Renewable Energy Laboratory, November 20-21, 2008.

6. X. Wang and R.K. Ahluwalia, "Dynamics of H_2S Poisoning of Pt Anodes in PEM Fuel Cells," Fuel Quality

Modeling Workshop, National Renewable Energy Laboratory, November 20–21, 2008.

7. R. Ahluwalia, D. Papadias, S. Lee, S. Ahmed, and H. Adachi, "Fuel Processor for Autothermal Reforming of Natural Gas for a Residential Fuel Cell System," 4th International Workshop on Hydrogen and Fuel Cells (WICaC 2008), Campinas, Sao Paulo, Brazil,, September 22–24, 2008.

8. X. Wang and R.K. Ahluwalia, "Dynamics of Poisoning of PEFC Pt-Anodes by CO and H_2S Impurities in Fuel H_2," 13th Meeting of ISO/TC197/WG12, CEA, Grenoble, France, February 3–4, 2009.

9. X. Wang, R.K. Ahluwalia and R. Kumar, "Performance of Automotive Fuel Cell Systems," Sixth IEA Annex XX Meeting, Argonne, IL, October 23–24, 2008.

10. X. Wang and R.K. Ahluwalia, "Effect of H_2S Impurity in Fuel Hydrogen on Performance of Polymer Electrolyte Fuel Cells," Fuel Cell Tech Team Meeting, Southfield, MI, August 19, 2008.

References

1. R.K. Ahluwalia, X. Wang, and R. Kumar, "Fuel Cell Systems Analysis," *2008 Hydrogen Program Review*, Arlington, VA, June 9–13, 2008.

2. M. Gee, Personal communications, 2009.

3. M.K. Debe and A.J. Steinbach, Personal communications, 2009.

4. Z.I. Mirza and V. Patel, Personal communications, 2009.